Fusion Engineering and Design 216 (2025) 115067

Contents lists available at ScienceDirect

Fusion Engineering and Design

journal homepage: www.elsevier.com/locate/fusengdes

Fluid-structural analysis of the IFMIF-DONES outlet channel during nominal operation

S. Gordeev [a,*], G. Verma [a], F.S. Nitti [b], J. Maestre [c]

[a] KIT, INR, Hermann-von-Helmhlotz-Platz 1, D-76344, Eggenstein-Leopoldshafen, Germany
[b] ENEA FSN-ING-SIS, C.R. Brasimone, I-40032, Camugnano, (BO), Italy
[c] IFMIF-DONES España, C/Gran Vía de Colón 48, E-18010, Granada, Spain

ARTICLE INFO

Keywords:
IFMIF-DONES
Lithium target
CFD
FEM
Fluid-structure interaction

ABSTRACT

The IFMIF-DONES (International Fusion Materials Irradiation Facility and DEMO—Oriented Neutron Source) facility relies on a single accelerator line to deliver 125 mA of deuteron at 40 MeV to a flowing liquid Lithium (Li) target, where the deuteron beam interacts with a free surface. The high-speed Li jet, reaching up to 15 m/s, must maintain a specific thickness to achieve the desired neutron flux and effectively dissipate heat. The performance of this jet is critical for designing key components, including the target assembly (TAA), nozzle, liquid Li channel, and quench tank (QT). Fluid-structural interaction simulations of the TAA outlet channel has revealed large oscillatory behaviour. This work analyses the dynamic characteristics of the TAA channel with outflowing liquid Li, using fluid-structure interaction simulations to understand and mitigate these oscillations. The scope of this study also extends towards understanding the vibrational effects of having a QT wall in the vicinity of the TAA outlet channel using coupled CFD-FEM simulations with a commercial code Siemens Star-CCM+. Further, the effect of stiffeners on the TAA channel towards decreasing amplitude of the vibratory behaviour is also studied. It has been observed that with increasing gap between the TAA outlet channel and the QT wall, the oscillatory behaviour becomes stable. Also, the stiffeners aid in reduction of the vibration amplitude.

1. Introduction

The IFMIF-DONES (the International Fusion Materials Irradiation Facility and DEMO—Oriented Neutron Source) facility is constructed to fulfil the requirements of a fast neutron-irradiation test facility for proposed European DEMO fusion reactors. It aims to test and characterize materials to be used in DEMO reactors under fast fusion neutron-like flux conditions. It utilizes a single accelerator line to supply 125 mA of deuteron at 40 MeV to a flowing liquid Li target (25 mm thick with cross-flow velocity of 15 m/s), where the deuteron beam faces a free surface. This high-speed of Li target is maintained to achieve the desired neutron flux and efficiently remove the released heat. Thus, the operational performance of the liquid Li jet governs the design of crucial components such as the target assembly (TAA), as well as all upstream and downstream components, including the nozzle, liquid Li channel, and quench tank (QT). Fig. 1 shows the design description of the crucial Li system components [1,2].

In the present work, the dynamic characteristics of the partially-immersed liquid Li discharging TAA outlet channel for a nominal DONES operation is investigated. Initial numerical investigation has revealed large oscillatory behaviour of the TAA outlet channel, which is partially immersed in liquid Li within the QT [3–5]. In the present study, this oscillatory behaviour and the effect of the QT wall in its vicinity is investigated. For this purpose, three sets of case studies involving fluid-structure interaction (FSI) simulations are performed using a commercial code Siemens Star-CCM+ [6] to understand the causes of the oscillatory behaviour of the channel. Also, the effect of the gap between the QT wall and the TAA channel on its vibration characteristics is estimated [7]. Further, the effect of longitudinal stiffeners on the TAA channel is also studied.

2. Computational domain

In this section, details of the computational domain such as the geometry, the grid system and the boundary conditions for the TAA outlet channel and the QT are described.

* Corresponding author.
E-mail address: sergej.gordeev@kit.edu (S. Gordeev).

https://doi.org/10.1016/j.fusengdes.2025.115067
Received 18 December 2024; Received in revised form 24 February 2025; Accepted 7 April 2025
Available online 18 April 2025

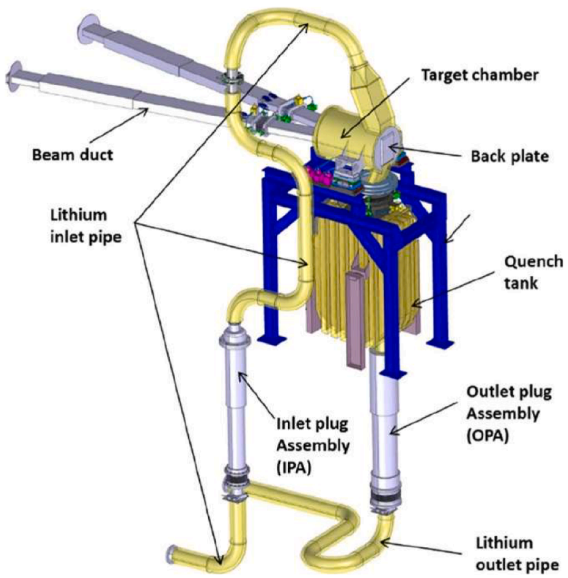

Fig. 1. Design description of the Target System of IFMIF-DONES [1].

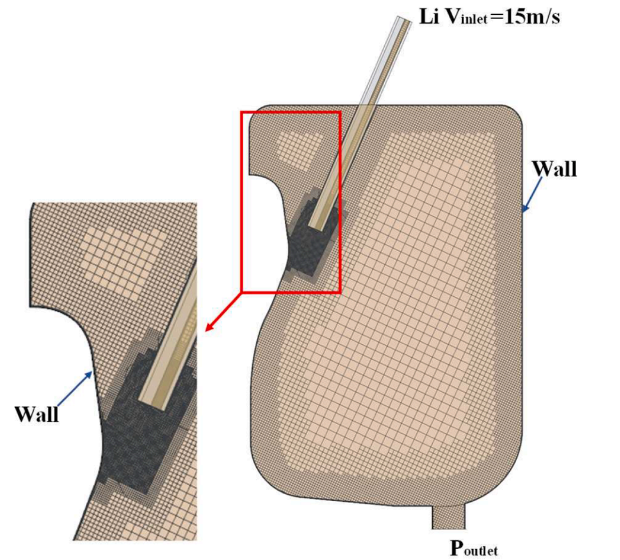

Fig. 3. Computational fluid domain and fluid boundary conditions for FSI analysis.

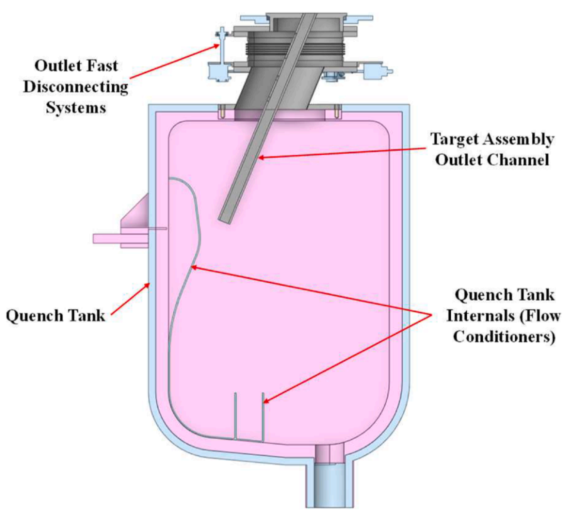

Fig. 2. Geometry of QT and TAA Outlet Channel.

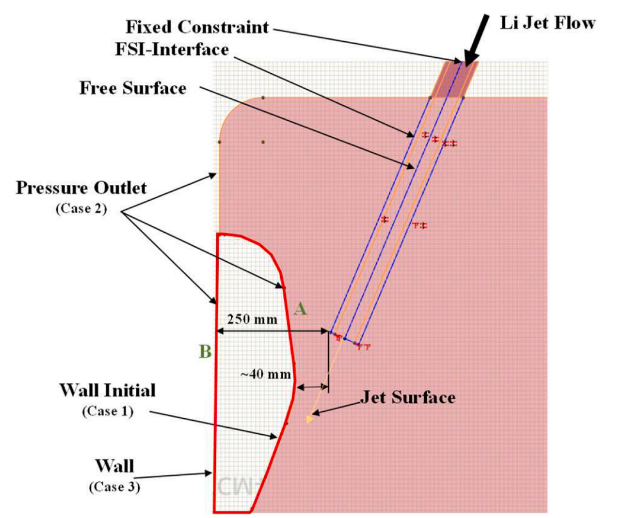

Fig. 4. Different boundary conditions for FSI analysis for different case studies.

2.1. Geometry

Fig. 2 shows the geometry of the computational domain. Liquid Li flowing at high velocity exits the TAA outlet channel in the form of a stable jet and is guided by the QT internals which directs the jet such that no direct impingement of the jet with QT wall occurs before its dissipation. The TAA outlet channel has a rectangular cross-section with outer dimensions 290 mm × 70 mm and inner dimensions of 260 mm × 50 mm and is inclined at an angle of 22.5° from the vertical. The inlet cross section is located in the connection area between the upper and lower flanges of the outlet channel assembly as shown if Fig. 2. At the free end, the gap between the channel and the flow conditioner wall of QT is 92.5 mm.

2.2. Grid system

The computational domain in the present work consists of the TAA outlet channel and the QT with its internal structures such as flow conditioners, etc. The TAA outlet channel structure is modelled with 1.99×10^6 unstructured tetrahedral cells and the fluid domain in the QT and TAA outlet channel with 8.5×10^6 unstructured trimmed cells. Near the walls, the fluid domain is modelled with 3 layers of tetrahedral cells. Unstructured mesh (trimmed cells oriented in channel flow direction) offer better flexibility for geometrically complex applications and are significantly less sensitive to strain. Fig. 3 displays the computational domain for the FSI analysis.

2.3. Boundary condition and material parameters

Figs. 3& 4 display the computational domain with fluid and structural domain boundary conditions respectively. From Fig. 3, it is seen that the Li inlet flow has a constant speed of 15 m/s. The walls of the QT are treated as no-slip wall condition and the boundary of the TAA channel is as fluid-structure interface. The free surface and outlet boundary is defined as pressure boundary. However, depending on the case study, the boundary conditions are slightly modified. Fig. 4 shows this variation for different case studies. For case study 1, the QT flow conditioner wall (shown as wall A in Fig. 4) is taken as the wall boundary with the TAA outlet channel free end in close vicinity which is also the current geometry of the QT. For the case study 2, the QT wall boundary

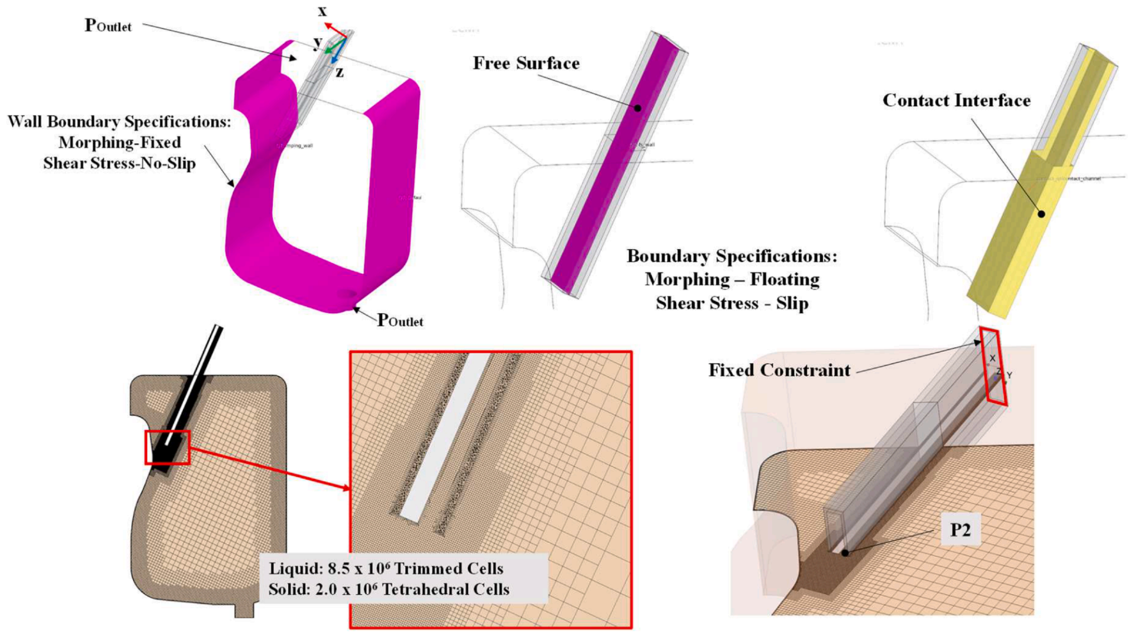

Fig. 5a. Boundary condition details for FSI analysis.

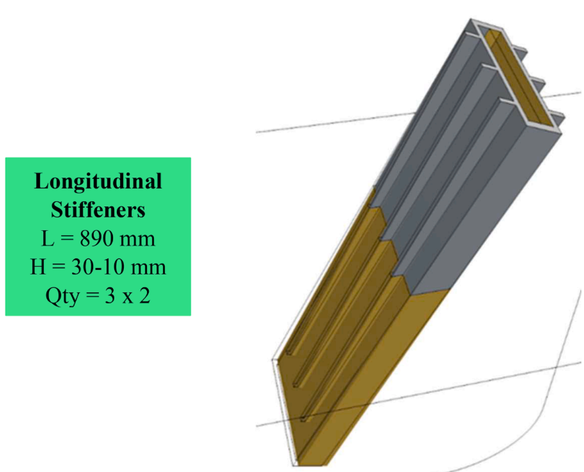

Fig. 5b. Geometry of the longitudinal stiffeners.

Table 1
Parameters used in the FSI simulations.

	Structural domain	Flow domain
Material	SS-316L	Liquid Li /Ar; (Two-phase flow)
Model assumptions	Constant density; Linear elastic low	Equation of state: Argon- constant density; Li- compressible; Li density ρ (p, c_s), $\rho_0 + p/c_s^2$ Li speed of sound c_0, 5000m/s Initial density ρ_0, 510 kg/m3 Li density pressure derivative ($d\rho/dp$), $1/c_0^2$

is treated as pressure outlet. And for case study 3, the flow conditioner wall (wall A) is removed and only the QT wall (wall B) exist such that the gap between the outlet channel and the wall is increased significantly.

The most commonly used, relatively robust k-ω Shear-Stress-Transport (SST) turbulence model is used for flow simulation. Because of different flow conditions in the near-wall regions the turbulence model is applied with automatic wall (all $y+$) treatment which allows for a smooth shift from a Low-*Re* (LR) number to a wall function formulation (High-Reynolds, HR) based on the near wall mesh spacing. This model allows the automatic switch of LR/HR treatment depending on the $y+$ value near the wall. Additionally, the model contains a new transport equation for the turbulent dissipation rate, which lets the model satisfy certain mathematical constraints on the normal stresses consistent with the physics of turbulence.

For FSI simulations, in the structural domain, the cross-sectional plane of the channel at the inlet is treated as a fixed boundary condition. Structural displacement motion allows the channel mesh to deform in real time based on the computed displacements. In the fluid domain, mesh morphing motion allows the fluid mesh to deform based on the displacements mapped at the interface. A single-phase model by treating the liquid Li-free-surface as a free-slip wall condition is considered. The floating wall boundary condition allows a small deformation of the wall surface induced by liquid inertial loads. A time-stepping of 10^{-4} s was utilized for the simulations. Fig. 5a shows the boundary condition details for the FSI simulation case studies and Fig. 5b displays the geometry of the longitudinal stiffeners. Table 1 describes the details regarding material properties used in the FSI simulations.

3. Dynamic characteristics of the TAA outlet channel

In order to investigate the dynamic characteristics of the partially-immersed liquid Li discharging TAA outlet channel, its characteristics in air needs to be investigated. After this evaluation, the outlet channel geometry can be simplified to perform more computationally intensive Fluid-Structure Interaction simulations to predict the dynamic behaviour in liquid Li.

3.1. Modal analysis of the TAA outlet channel

In this section, dry and wet modal analysis of the TAA outlet channel geometry (shown in Fig. 4) is performed in a commercial code (ANSYS 2023 R2). The bellow which connects the QT to the TAA outlet channel through Outlet Fast Disconnecting Systems (FDS) has axial stiffness of 14.55 MN/m (as per EJMA), however, in the present work for simplicity and understanding the large computational time for multiple FSI case studies, in the preliminary investigation, it is assumed that bellow

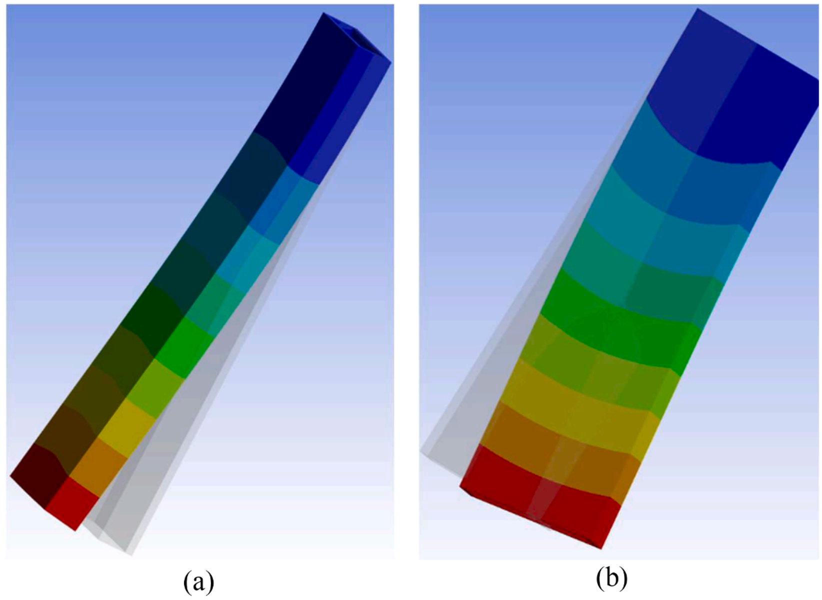

Fig. 6. Dry and wet modes of TAA channel (a) 1st mode (b) 2nd mode.

Table 2
Natural frequencies of the TAA outlet channel for dry and wet modal analysis.

Mode No	Dry	Wet
1	75.1 Hz	67.63 Hz
2	251.9 Hz	227.1 Hz

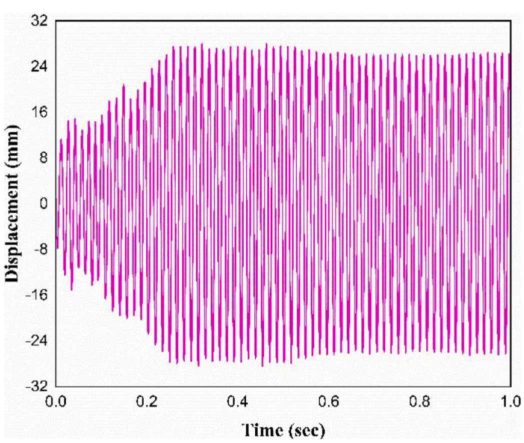

Fig. 7. Response of TAA outlet channel in terms of displacement vs time (case study-1; cond.1).

shown has very high stiffness resulting in rigid connection between the QT and the TAA outlet channel.

For wet modal analysis, added mass is analytically calculated for the TAA channel and implemented in the model in the form of increased density of the channel. In this analytical calculation, the added mass effects due to the internal half-filled Li and externally partially immersed Li is considered. Fig. 6 shows the first two dry and wet modes of the TAA outlet channel. Table 2 describes the first two natural frequencies of the TAA outlet channel for dry and wet modes.

4. Results and discussion

As discussed earlier, initial numerical investigation of the TAA outlet channel has revealed large oscillatory behaviour while discharging Li at

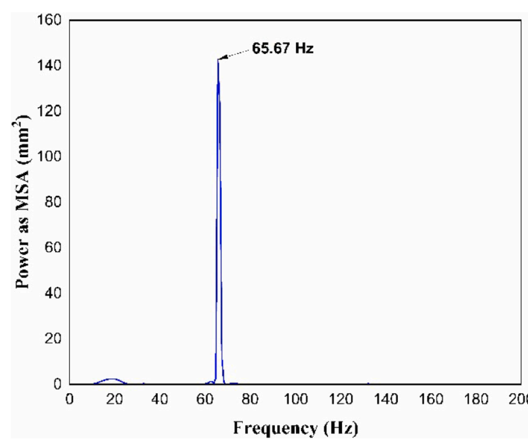

Fig. 8. FFT of TAA outlet channel response (case study-1; cond.1).

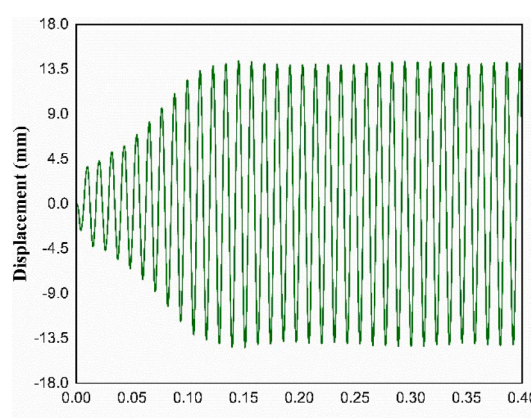

Fig. 9. Response of TAA outlet channel in terms of displacement vs time (case study-1; cond.2).

high velocities within the QT. In this section, this oscillatory behaviour of the TAA outlet channel and the effect of the QT wall in its vicinity is investigated with the help of three sets of case studies involving FSI

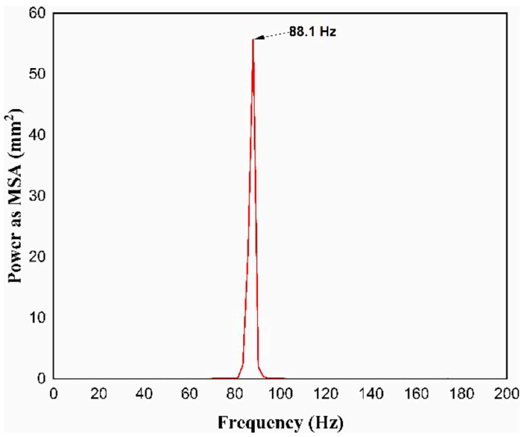

Fig. 10. FFT of TAA outlet channel response (case study-1; cond.2).

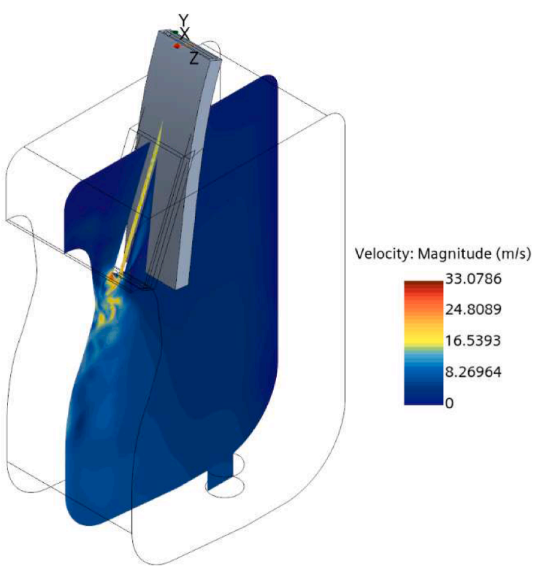

Fig. 11. Velocity contour of the discharging fluid for case study-1: condition-1.

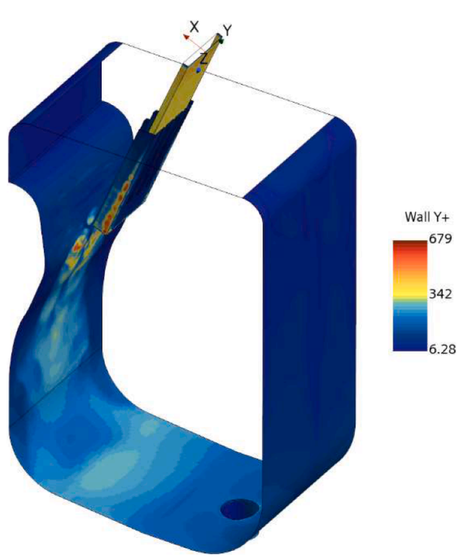

Fig. 12. Wall Y^+ distribution for case study-1: condition-1.

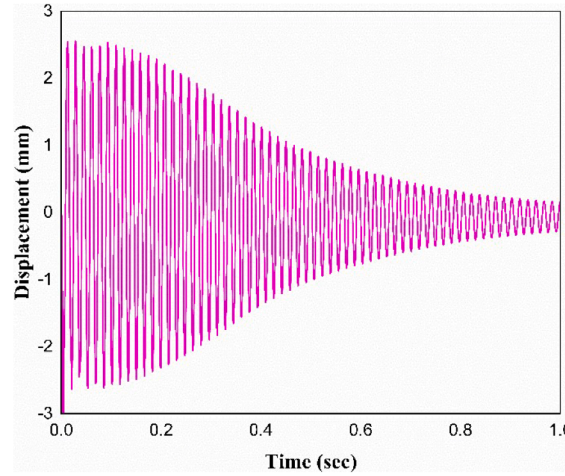

Fig. 13. Response of TAA outlet channel in terms of displacement vs time (case study-2; cond.1).

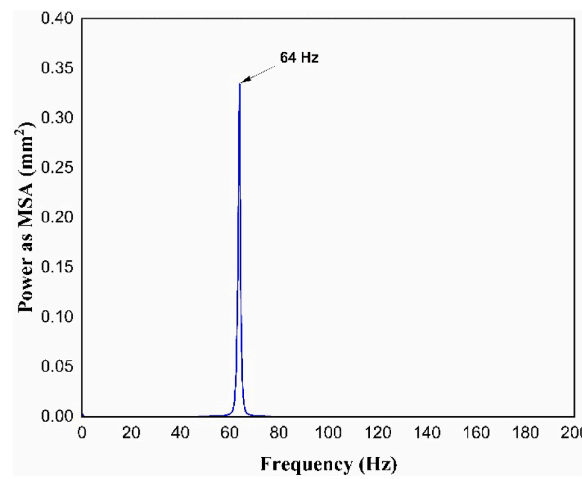

Fig. 14. FFT of TAA outlet channel response (case study-2; cond.1).

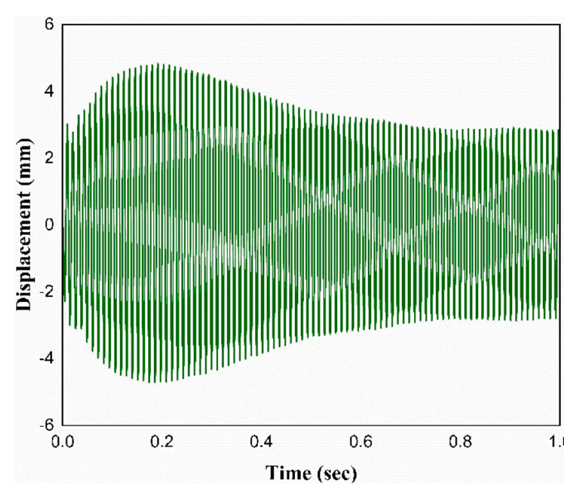

Fig. 15. Response of TAA outlet channel in terms of displacement vs time (case study-2; cond.2).

simulations. These are carried out to understand the cause of the oscillatory behaviour of the channel. In addition, the effect of longitudinal stiffeners on the TAA channel is also studied.

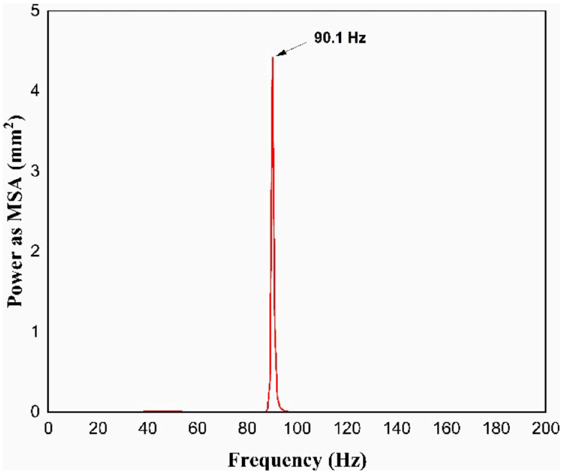

Fig. 16. FFT of TAA outlet channel response (case study-2; cond.2).

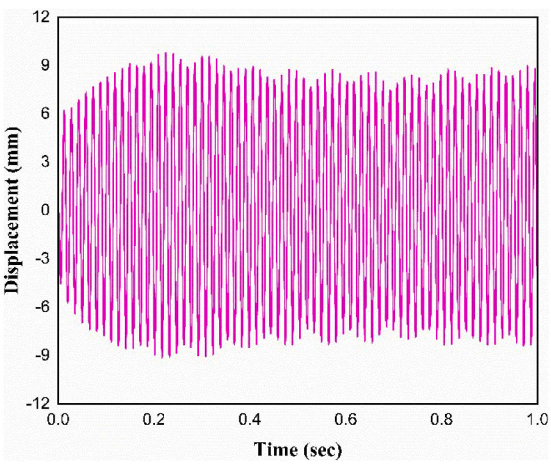

Fig. 17. Response of TAA outlet channel in terms of displacement vs time (case study-3; cond.1).

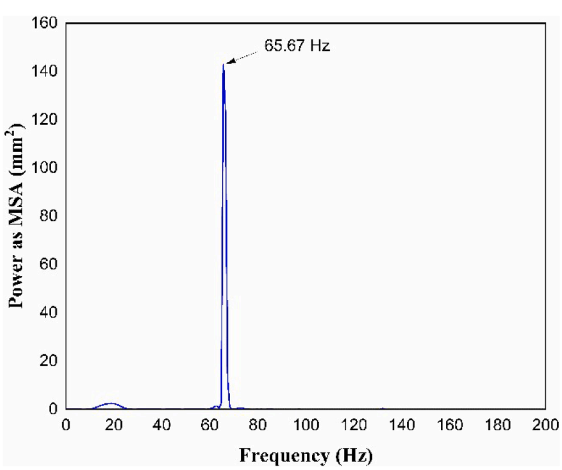

Fig. 18. FFT of TAA outlet channel response (case study-3; cond.1).

4.1. Case study 1

In this case study, the current geometry of the TAA outlet channel and QT is simulated with and without stiffeners as two different conditions respectively. For this case study, the QT flow conditioner wall

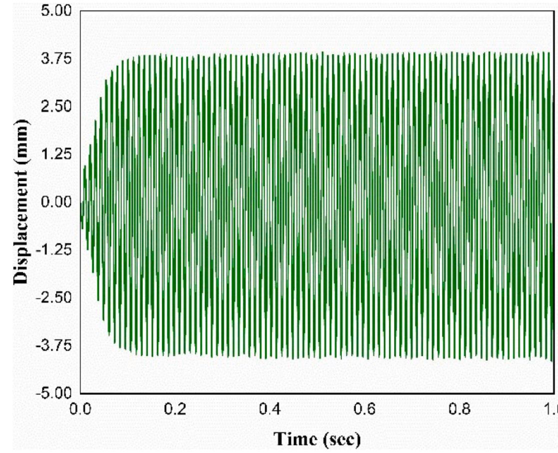

Fig. 19. Response of TAA outlet channel in terms of displacement vs time (case study-3; cond.2).

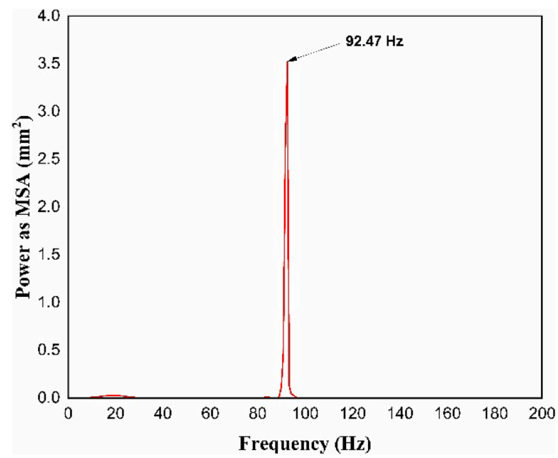

Fig. 20. FFT of TAA outlet channel response (case study-3; cond.2).

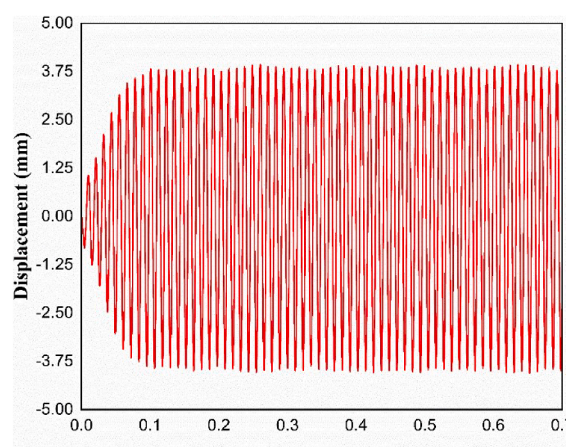

Fig. 21. Response of TAA outlet channel in terms of displacement vs time (case study-3; cond.3).

(shown as wall A in Fig. 4) is chosen as the wall boundary with outlet channel free end in close proximity.

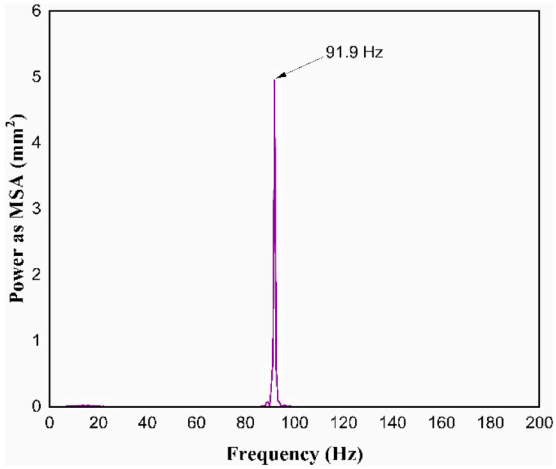

Fig. 22. FFT of TAA outlet channel response (case study-3; cond.3).

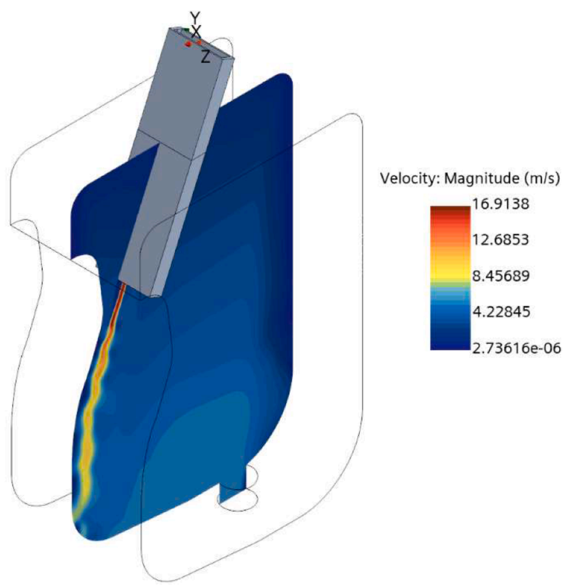

Fig. 23. Velocity contour of the discharging fluid for case study-2: condition-1.

4.1.1. Condition 1

For this condition, the current geometry of the outlet channel and the QT is simulated. Fig. 7 shows the temporal variation of the free end displacement of the outlet channel with time. Fig. 8 shows the Fast Fourier Transformation (FFT) of the displacement vs time signal shown in Fig. 7. From Fig. 7, it is observed that the displacement amplitude of the channel initially grows and then becomes stable with displacements of ±26 mm. Also, from FFT shown in Fig. 8, the flow induced frequency in first bending mode of the partially immersed discharging outlet channel is 65.67 Hz which is in close agreement with the first wet mode frequency shown in Table 2. Fig. 11 shows the velocity contour of the fluid. The maximum velocity of the jet observed is 33 m/s. Fig. 12 displays the wall y^+ value for this condition.

4.1.2. Condition 2

In order to reduce the vibration amplitude of the TAA outlet channel, longitudinal stiffeners are attached to it. As can be seen from Fig. 9, because of this increased stiffness of the channel, the displacement amplitude has almost reduced by half and as expected, the natural frequency of the channel has increased significantly to 88.1 Hz as displayed in FFT in Fig. 10. However, the displacement trend is still the same as

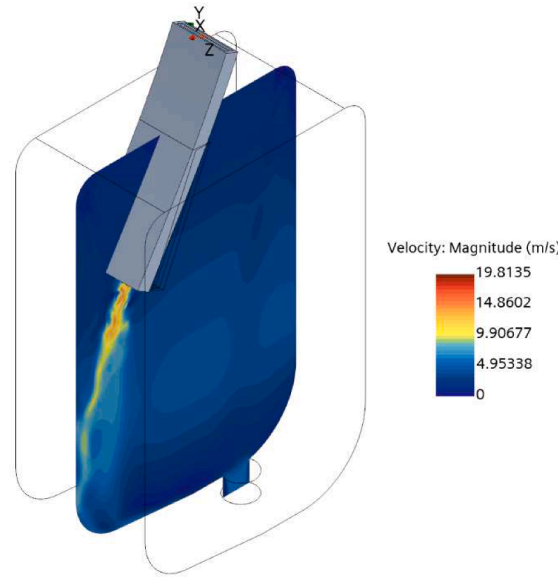

Fig. 24. Velocity contour of the discharging fluid for case study-3: condition-1.

described for Condition 1. Here also, it is observed that the displacement amplitude initially grows and then stabilizes.

4.2. Case study 2

In this case study, in order to understand the effects of the boundary condition, the QT wall boundary is treated as pressure outlet. This resembles a situation where there are no wall effects on the dynamic characteristics of the outlet channel and no interaction of the channel with the rebounded liquid from the walls. For this case study also, two different conditions i.e., outlet channel with and without stiffeners are simulated.

4.2.1. Condition 1

For this condition, the current geometry of the outlet channel without stiffeners is simulated. Fig. 13 shows the variation of displacement of the outlet channel and Fig. 14 displays the FFT of the displacement-time. From Fig. 13, it is observed that in the absence of wall effects, displacement of the channel decays with time with initial maximum displacement of ±2.5 mm. From FFT shown in Fig. 14, the flow-induced first wet frequency for this condition is 64 Hz which is slightly lower than in the case study 1. Fig. 23 shows the velocity contour of the fluid for this condition where the maximum velocity of the jet observed is also reduced to 16.9 m/s. This implies that presence and absence of a wall affects both the vibration characteristics of the outlet channel as well as the characteristics of the jet.

4.2.2. Condition 2

In order to further investigate the effects of the stiffeners, in this condition in which longitudinal stiffeners are joined to the outlet channel is analysed. As seen from Fig. 15, because of this increased stiffness of the channel, the displacement amplitude has increased unexpectedly instead of reducing as compared to the previous case study, however, the stiffness has increased which is expected. The wet natural frequency of the channel has increased to 90.1 Hz (Fig. 16). Also, the decaying displacement trend is duplicated by this condition however, rate of decay has reduced significantly.

4.3. Case study 3

In this last case study, the effects of the QT wall boundary proximity on the dynamic characteristics of the outlet channel are investigated.

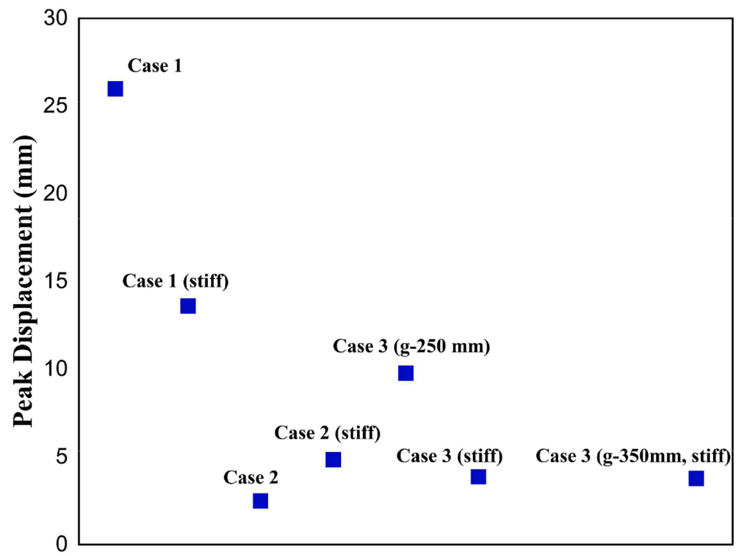

Fig. 25. Peak displacement for different case studies.

This case study consists of two conditions for analysis. In condition-1, the QT flow conditioner wall boundary is removed and instead of that, the vertical wall of the QT (shown in Fig. 4) is considered as the wall boundary such that the gap between the wall and the discharging end of the channel now has a gap of 250 mm. For condition-2, longitudinal stiffeners are modelled on the outlet channel. For condition-3, the vertical wall of the QT is further shifted away from the TAA channel by 100 mm, such that the gap between wall and the channel has increased to 350 mm. Also, for this condition, the stiffeners are modelled on the outer channel.

4.3.1. Condition 1

For this condition, instead of QT flow conditioner wall, the vertical QT boundary is assumed to be the wall boundary and the minimum gap between outlet channel and vertical wall boundary is 250 mm. Fig. 17 shows the displacement variation of the outlet channel and Fig. 18 displays its FFT. From Fig. 17, it is observed that as the gap between the channel and wall is increased, the amplitude of the displacement has reduced significantly compared to case study-1 condition-1 with ±9 mm though the displacement trend is similar with initial growth and subsequent sustenance [6]. As expected, the frequency of the vibrating channel is still 65.67 Hz as shown in Fig. 18. From Fig. 24, it can also be seen that the peak jet velocity has reduced to 19.8 m/s. As implied earlier, proximity of a wall affects both the vibration characteristics of the outlet channel as well as the characteristics of the jet.

4.3.2. Condition 2

In this condition, the added stiffening effects of the longitudinal stiffeners is investigated. As seen in Fig. 19, with increased stiffness of the channel, the maximum displacement amplitude has reduced significantly to ±3.9 mm. Also, from Fig. 20, a frequency of 92.47 Hz is observed which is slightly higher compared to Condition 2 of Case Study 1.

4.3.3. Condition 3

In this condition, the gap between the vertical wall of the QT and the TAA channel is increased to 350 mm by shifting the QT walls away from the channel by 100 mm. As seen in Fig. 21, not much reduction in the vibration amplitude of the channel is observed. From Fig. 22, a wet flow induced frequency of 91.9 Hz for the stiffened TAA channel is observed which is in close agreement with the frequency in Condition 2. Fig. 25 shows the Peak displacement for different case studies.

5. Conclusion

In the present work, results of analyses of dynamic characteristics of TAA channel with discharging liquid Li, using FSI simulations was presented. The scope of the present work also extended towards understanding vibrational effects of having QT wall in proximity to TAA channel. Effect of longitudinal stiffeners on TAA channel towards decreasing amplitude of the vibratory behaviour was also studied. Three sets of case studies with different boundary conditions were performed to understand the causes of oscillatory behaviour of TAA channel. It was observed that all the case studies except the case study involving pressure-outlet boundary condition on the QT wall behaved consistently as expected. The reason for the inconsistency by the case study can be explored in future works. It was observed that with increasing gap between the TAA outlet channel and the QT wall, the oscillation amplitude of the channel decreases up to a certain limit. Also, the longitudinal stiffeners further aid in reduction of the vibration amplitude.

In upcoming studies, the effect of the free surface of liquid Li in the QT with the help of two-phase flow simulations on the dynamic characteristics of TAA outlet channel will be investigated. In order to define the boundary conditions more realistically, the model will be extended to the Li target structure. The fastening elements such as connecting flanges and bellows will be also included in the simulations.

CRediT authorship contribution statement

S. Gordeev: Investigation. **G. Verma:** Investigation. **F.S. Nitti:** Investigation. **J. Maestre:** Investigation.

Declaration of competing interest

The authors declare that they have no known competing financial interests or personal relationships that could have appeared to influence the work reported in this paper.

Acknowledgments

This work has been carried out within the framework of the EUROfusion Consortium, funded by the European Union via the Euratom Research and Training Programme (Grant Agreement No 101052200 — EUROfusion). Views and opinions expressed are however those of the author(s) only and do not necessarily reflect those of the European Union or the European Commission. Neither the European Union nor the

European Commission can be held responsible for them

Data availability

No data was used for the research described in the article.

References

[1] S. Gordeev, et al., Thermal hydraulic and structural analysis of the IFMIF-DONES liquid-lithium target system, Nucl. Mater. Energy 40 (2024) 101689.
[2] S. Gordeev, et al., Numerical study of the flow conditioner for the IFMIF liquid lithium target, Fusion Eng. Des. 89 (2014) 1751–1757.
[3] M.J. Hannoyer, M.P. Paidoussis, Instabilities of tubular beams simultaneously subjected to internal and external axial flows, Trans. ASME 100 (1978) 328–336.
[4] M.P. Paidoussis, N.T. Issid, Dynamic stability of pipes conveying fluid, J. Sound Vib. 33 (3) (1974) 267–294.
[5] H.Y. Min, Natural frequency analysis of fluid conveying pipeline with different boundary conditions, Nucl. Eng. Des. 240 (2010) 461–467.
[6] SiemensDigital Industries Software. Simcenter STAR-CCM+ 2402.
[7] G. Verma, et al., Fluid-structure coupled vibration characteristics of liquid immersed square channels within confinement, Ann. Nucl. Energy 172 (2022) 109061.